Research Article | Vol. 28, No. 23 / 9 November 2020 / Optics Express 34390
Optics EXPRESS

LED primary selection algorithms for simulation of CIE standard illuminants

ALIREZA MAHMOUDI NAHAVANDI,[1,*] MAHDI SAFI,[2] POUYA OJAGHI,[3] AND JON YNGVE HARDEBERG[4]

[1]*Color Imaging and Color Image Processing Department, Institute for Color Science and Technology (ICST), Tehran, Iran*
[2]*Department of Color Physics, Institute for Color Science and Technology (ICST), Tehran, Iran*
[3]*Elite Engineers Corporation, Tehran, Iran*
[4]*Department of Computer Science, NTNU - Norwegian University of Science and Technology, Gjøvik, Norway*
[*]*amahmoodi@icrc.ac.ir*

Abstract: Although mixture of LEDs is being considered as a simulator of the CIE daylight series, the performance of the simulations is highly dependent on the SPD of the selected LEDs. An algorithm for selection of the best LEDs for simulation of the CIE daylight series is helpful in this regard. To address this problem, using 200 imaginary light primaries and 40 real LEDs, three algorithms based on concepts of equally spacing of wavelength range ("Equal"), Gram Schmidt orthogonalization in LEDs/light primaries spectral subspace ("Gram") and the generalization of Gram Schmidt orthogonalization in the LEDs/light primaries projections onto the illuminants subspace ("Ortho") were proposed and studied. Algorithms, in simulation and reality, were implemented for the CIE standard illuminants of D50, D55, D65 and D75, C and A. The results showed that the performance of the proposed algorithms generally increase with the higher number of selected LEDs/light primaries, while for the LEDs "Gram" and "Ortho" methods showed superior performance, simulations on the imaginary light primaries showed "Ortho" could be considered as the best algorithm.

1. Introduction

The spectral power distribution (SPD) of manmade light sources is an important factor that influences human color perception. Standard illuminants defined by the International Commission on Illumination (CIE) play an important role for standardization and communication of color. CIE standard illuminant simulators, for instance in the form of light booths, are frequently used in various color-critical industries such as graphic arts or textile industry. However, it is a fact that their spectral power distribution are generally far from the standardized illuminants, since they are typically based on fluorescent light tubes, tungsten lamps, and colored filters. Customers and users are generally referred to metrics like Correlated Color Temperature (CCT) and Color Rendering Index (CRI) as the only information about the light sources.

Light Emitting Diode (LED) lights, since their emergence, have today come a long way to become a light source to be counted on, rather than a dim indicator signal. High-intensity blue emitters coated with a yellow phosphor have found their ways into home and automotive lightings [1]. Meanwhile, there are demands for use these sources of light in exit signs, traffic lights, decorative lighting, nightlights and neon-replacements [1].

Despite companies' efforts on the satisfaction of CRI requirements for white LED light sources, the SPD of these white LEDs are by far different from their corresponding black body radiators [2]. Cool daylight simulators of light cabinets as an industrial solution for daylight simulation are also just an approximation of daylight with CIE F7 [3].

#408754 https://doi.org/10.1364/OE.408754
Journal © 2020 Received 7 Sep 2020; revised 17 Oct 2020; accepted 18 Oct 2020; published 28 Oct 2020

Optics EXPRESS

Although it is almost impossible to manufacture a LED with a single light emitter chip for matching some desired SPD, from a color modeling point of view [4], a combination of different LEDs could be used for simulation of any spectrum. The different LEDs can be regarded as a color primaries, and rules of additive color mixing can be employed [5].

It is worth noting that despite some companies claims for production of single chip high CRI LEDs they are just matter of experimental design and might have divergence from what has been promised in the models [6]. Moreover, unlike the approach presented in the current study, one arrangement of chip-phosphor can only simulate one specific SPD.

Although there are some papers working on the spectral matching of the CIE illuminants [1,7–12], to the authors' knowledge, only very few papers have addressed the selection of the best set of LEDs for their simulations [10–12]. The subject is important as for a few dozen of available LEDs, there would be billions of possible combinations for controlling their performance.

Lei et al. [13] worked on optimization of luminous efficiency of white light sources made up of some theoretical LEDs while maintaining CRI and CCT. Using a fitting technique they presented a function for prediction of luminous efficiency of mixed LED based theoretical light source for an assumed CCT and CRI.

Papoulis [14] showed that mean vector of some random vectors is the least square solution of distance from the random vectors. Based on this theorem, Hu et al. [11] considered daylight series as random vectors and the mean vector was considered as the target of matching for optimally selected LEDs in order to reconstruct daylight series. Using linear algebraic models and finding an upper boundary for the reconstruction error and then utilizing minimax technique, LED selection was carried out using pruning process from an available LED dataset. However, the authors did not give any answer to the question of whether minimizing the distance from the mean vector does indeed guarantee minimization of distance from all studied random vectors.

The pruning technique was also utilized by Wu et al. [10] using a different pruning metric and taking advantage of the same strategy of optimizing for the mean vector [11,14] and then continued for energy flux optimization in addition to SPD matching [12].

Inspired by a work by Hardeberg [15,16] for selection of best transmission colored filters for spectral estimation, we propose and study three methods for selection of best set of LEDs.

The first is the Gram-Schmidt orthogonalization algorithm [17]. This algorithm argues that spaces can be covered using set of orthogonal bases. The set of desired CIE standard illuminants make a subspace and this subspace should thus be covered with the selected LEDs. From a coverage point of view, the best set would then be the one with the most orthogonal LEDs.

The second method is maximizing orthogonality in the target illuminants subspace. This method selects LED SPDs that possess projection vectors onto the target standard illuminants subspace with high degree of orthogonality. In other words, this method is the generalization of Gram-Schmidt orthogonalization on the vector of the projection of selected LEDs on the CIE illuminants subspace. In fact, it looks for the most significant primaries that are different from what has already been selected.

The last method is the obvious notion of choosing LEDs such that central wavelengths are approximately equally spaced within the visible spectrum.

This paper is organized as follows. At first the mathematics of the proposed methods is presented. After that, using 200 simulated light primaries generated using mixture of Gaussian functions, the proposed ideas were tested and controlled. Then, using 40 LEDs, a controller and a custom made integrating sphere, the proposed algorithms were tested on the 40 LEDs in simulation and reality. Finally, the results of the optimization are interpreted and justified.

Throughout the paper lowercase boldface letters represent vectors, uppercase boldface letters are used for matrices, and regular letters indicate scalars.

Optics EXPRESS

2. Mathematical background of proposed methods

2.1. Gram-Schmidt orthogonalization ("Gram")

Simulation of a light spectrum with some additive primaries could be done if the primaries have enough power in the spectral space of the standard illuminants. The selection of basis for covering spaces could be done via Gram-Schmidt orthogonalization algorithm as decribed below.

If $[\mathbf{b}_1, \ldots, \mathbf{b}_k]$ is a basis for $\Re^n$ then

$$\begin{aligned}
\mathbf{u}_1 &= \mathbf{b}_1. \\
\mathbf{u}_2 &= \mathbf{b}_2 - proj_{\mathbf{u}_1}(\mathbf{b}_2). \\
\mathbf{u}_3 &= \mathbf{b}_3 - proj_{\mathbf{u}_1}(\mathbf{b}_3) - proj_{\mathbf{u}_2}(\mathbf{b}_3). \\
&\ldots \\
\mathbf{u}_k &= \mathbf{b}_k - proj_{\mathbf{u}_1}(\mathbf{b}_k) - \ldots - proj_{\mathbf{u}_{k-1}}(\mathbf{b}_k).
\end{aligned} \tag{1}$$

$[\mathbf{u}_1, \ldots, \mathbf{u}_k]$ forms a an orthogonal basis for the same subspace. In Eq. (1) $proj_{\mathbf{x}}(\mathbf{y}) = \{\mathbf{x}(\mathbf{x}^t\mathbf{x})^{-1}\mathbf{x}^t\}\mathbf{y}$ and the superscript t denotes transpose of a vector or matrix.

Now let's assume a set of LEDs/light primaries is going to simulate some illuminants. This is as if these LEDs/light primaries should be bases for the desired illuminants subspace. So, implementation of Gram-Schmidt orthogonalization algorithm for selection of LEDs for the problem is as below:

The first LED/light primary ($\mathbf{l}^1$) is the one with the maximum power. Selection is done as shown in Eq. (2) and superscripts indicate selections.

$$\mathbf{l}^1 = \arg\max_i^{i=1..k} ||\mathbf{l}^i||. \tag{2}$$

$||\mathbf{x}||$ indicates the 2-norm of the vector $\mathbf{x}$. The second LED/light primary ($\mathbf{l}^2$) is selected such that:

$$\mathbf{l}^2 = \arg\max_i^{i=2..K} ||\mathbf{l}^i - (\mathbf{l}^1(\mathbf{l}^{1^t}\mathbf{l}^1)^{-1}\mathbf{l}^{1^t})\mathbf{l}^i||. \tag{3}$$

Note that Eq. (3) is the implementation of second line of Eq. (1).

Selection of LED/light primary with the maximum projection difference guarantees the selection of the spectrally most orthogonal LED/light primary to the selected ones for better spanning of the target illuminants subspace. In other words, Eq. (3) approximates the second step of gram-Schmidt orthogonalization algorithm.

Other LEDs/light primaries are selected according to Eq. (4). such that :

$$\begin{aligned}
&\mathbf{l}^{k+1} = \arg\max_i^{k<i\leq K} ||\mathbf{l}^i - \mathbf{L}^k(\mathbf{L}^{k^t}\mathbf{L}^k)^{-1}\mathbf{L}^{k^t}\mathbf{l}^i||. \\
&\textit{such that}: \ \mathbf{L}^k = [\mathbf{L}^{k-1}\ \mathbf{l}^k].
\end{aligned} \tag{4}$$

It could be easily seen that Eq. (4) is implementation of last line of Eq. (1).

For better illustration of the applying Gram-Schmidt orthogonalization algorithm for the selection of LEDs, the geometrical interpretation of the selections steps for four assumed LEDs are shown in Fig. 1. In this figure desired standard illuminants is shown as STD vector. The 3 thick axes of short, medium and long wavelengths are representative of the visible spectral space. As the LEDs vector lengths are the criterion for the first step of the algorithm, LED 4 with the length of 19.0000 is the result of the first step as shown in Fig. 1(a). LED 3 with the projection length of 15.4416 on LED 4 is the second selection (Fig. 1(b)). The LED 4 and LED 3 make a spectral subspace as shown with cyan bricks hatched plane in Fig. 1(c). LED 2 with the distance of 7.9292 from aforementioned subspace is the results of third step of the selection algorithm.

Optics EXPRESS

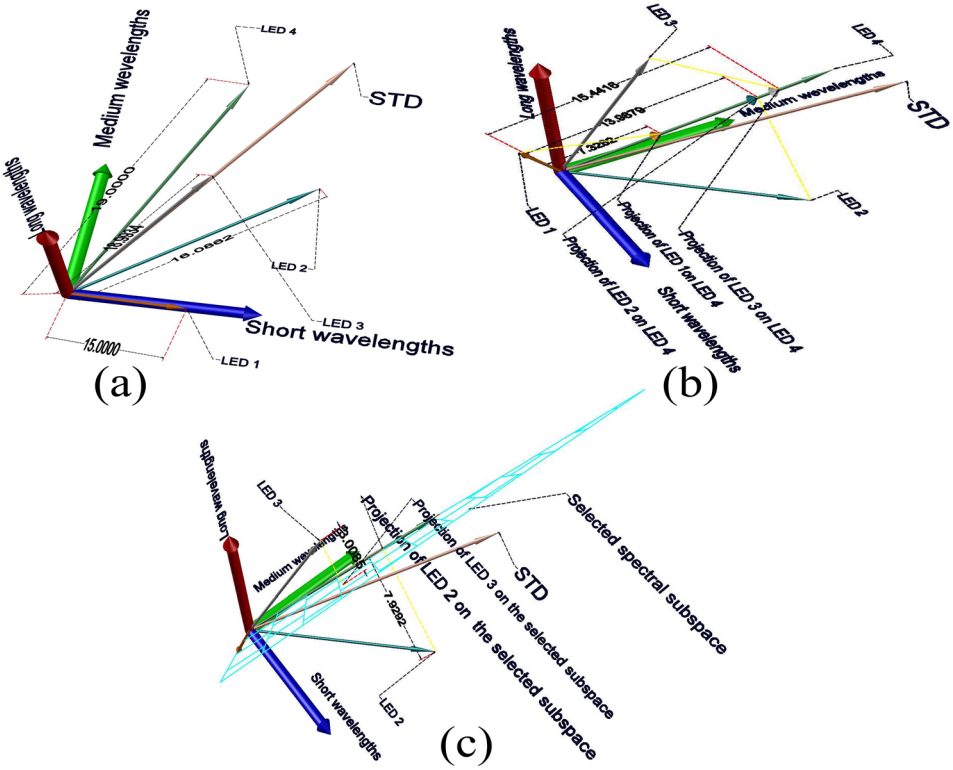

Fig. 1. Geometrical illustration of Gram-Schmidt orthogonalization in the spectral space. STD is the subspace of the desired CIE standard illuminants. Dimensions of the spectral space are shown with the thick vectors in blue, green and red with the labels short wavelengths, medium wavelengths and long wavelengths, respectively. The first, second and the third steps are shown in (a), (b) and (c), respectively.

2.2. *Maximizing orthogonality on the target illuminants subspace ("Ortho")*

Let's assume that the matrix of the desired standard illuminants (**STD**) is decomposed by singular value decomposition algorithm as shown in Eq. (5).

$$\mathbf{STD} = \mathbf{U}_{n_w.n_w}\mathbf{S}_{n_w.n_r}\mathbf{V}_{n_r.n_r}. \tag{5}$$

Where, n_w is the number of wavelengths and n_r is the number of singular values of **STD**.

In this selection algorithm the first LED/light primary is selected such that it possess maximum of power after projection onto the target illuminants subspace as shown in Eq. (6). Selection of the LED/light primary with the maximum power at the first step would be a wise criterion as it helps the simulated SPD have enough power in the target standard illuminants subspace.

$$\begin{aligned} &\mathbf{P}_{n_w n_{LEDs}} = \mathbf{U}_{n_w n_w}\mathbf{L}_{n_w n_{LEDs}}, \mathbf{p}_{n_w 1} = \mathbf{U}_{n_w n_w}\mathbf{l}_{n_w 1}. \\ &\mathbf{l}^1 = \arg\max_i^{i=1..K}(||\mathbf{p}||), \ \mathbf{p}^1 = \mathbf{U}\mathbf{l}^1. \end{aligned} \tag{6}$$

Where, n_{LEDs} is the number of available LEDs/light primaries.

Optics EXPRESS

The second LED/light primary is the one whose projection of the target standard illuminants on it is the most orthogonal relative to $\mathbf{p}^1$ as shown in Eq. (7).

$$\begin{aligned} &\mathbf{l}_1 = \arg\max_i^{i=2..K}(\mathbf{p}^i - (\mathbf{p}_n^1(\mathbf{p}_n^{1^t}\mathbf{p}_n^1)^{-1}\mathbf{p}_n^{1^t})\mathbf{p}^i)\,. \\ &,\ \mathbf{p}_n^j = \frac{\mathbf{p}^j}{||\mathbf{p}^j||}, j = 1..K. \end{aligned} \tag{7}$$

Next LEDs/light primaries are selected such that:

$$\begin{aligned} &\mathbf{l}^{k+1} = \arg\max_i^{k<i\leq K} ||\mathbf{p}^i - (\mathbf{P}_n^k(\mathbf{P}_n^{k^t}\mathbf{P}_n^k)^{-1}\mathbf{P}_n^{k^t})\mathbf{p}^i||. \\ &\textit{such that}:\ \mathbf{P}_n^k = [\mathbf{P}_n^{k-1}\mathbf{p}_n^k]\,. \\ &\textit{and}\ \ \mathbf{p}_n^k = \frac{\mathbf{p}^k - (\mathbf{P}_n^{k-1}(\mathbf{P}_n^{k-1^t}\mathbf{P}_n^{k-1})^{-1}\mathbf{P}_n^{k-1^t})\mathbf{p}^k}{||\mathbf{p}^k - (\mathbf{P}_n^{k-1}(\mathbf{P}_n^{k-1^t}\mathbf{P}_n^{k-1})^{-1}\mathbf{P}_n^{k-1^t})\mathbf{p}^k||}. \end{aligned} \tag{8}$$

For geometrical illustration of the "Ortho" algorithm, the steps of the selections for the four assumed LEDs are shown in Fig. 2. The length of projections of the 4 LEDs on the STD subspace is shown in Fig. 2(a). It can easily be seen that LED 4 is the winning candidate with the projection length of 18.7243. Projection location of the other 3 LEDs on the standard illuminants subspace should be compared with the first selection for the second step of the algorithm. The second selection is LED 1 as shown in Fig. 2(b). Either LED 2 or LED 3 are both the winner of the third step as their projection length is zero on the selected spectral subspace made by projections of the LED1 and LED 4 on the STD. It is worth noting that the similarity of the selection results of LED 4 and LED 1 for the first and the second steps with the algorithm "Gram" is completely accidental and can be easily changed with different orientations of LEDs with respect to the STD. For two or three of standards, the STD vector would become to a surface and volume, respectively and the projection of the available LEDs on the Eigen vectors of on the standards subspace would pass through steps of the algorithm.

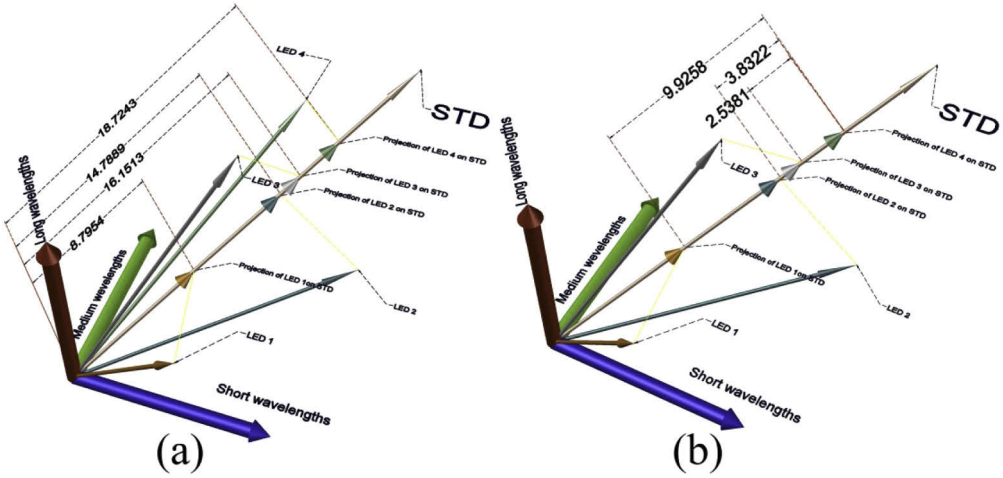

Fig. 2. Geometrical illustration of "Ortho" algorithm in the spectral space. STD is the subspace of the desired CIE standard illuminants. Dimensions of the spectral space are shown with the thick vectors in blue, green and red with the labels short wavelengths, medium wavelengths and long wavelengths, respectively. The first, second steps are shown in (a) and (b) respectively.

Optics EXPRESS

2.3. LED/light primary selection with peaks located in an equally divided visible spectrum ("Equal")

In this method the studied wavelength range is equally divided into the desired number of LEDs/light primaries. For each division, the LED/light primary with the nearest peak to the center of the division is selected so that the studied wavelength range is covered. For the phosphor coated LEDs/multiple peaks light primaries, the highest peak is considered as the peak of the LED/light primary. From the vector space point of view "Equal" algorithm behaves similar to "Gram" provided selection is forced from some narrow band LEDs. This is due to the fact that difference in the peak wavelengths means maximization of the spectral difference as it was shown in Fig. 1.

3. Experimental

In order to test the 3 proposed selection algorithms, two approaches were pursued. The first is to use some imaginary light primaries and applying the algorithms for these primaries. The second is to apply the algorithms for a set of 40 real LEDs to check the performance of the algorithms in reality. These approaches are fully described in detail in sections 3.1 and 3.2, respectively.

After the selection of the LEDs/imaginary light primaries, their intensities should be tuned via an optimization technique so that some desired standard illuminants are matched. CIE illuminants of A, C, D50, D55, D65 and D75 were used as the target standard illuminants. Eigen vectors of the target standard illuminants data set showed that the intrinsic dimensionality [15] of the dataset for 99.999% of cumulative variance is 4. So, four Eigen vectors were used for estimation of the illuminants for "Ortho" method.

In order to perform matching of the target standard illuminants, the Genetic algorithms in MATLAB optimization toolbox were used for the optimizations. Optimization parameters were considered as the default values except population size, that were 10 times increased to 200 individuals. Moreover, reaching to 150 generation was added to the list stopping criteria. In order to have a hybrid optimization, constrained nonlinear optimization (fmincon) was also utilized to make sure to not to get stuck in local optimums. This is as if the Genetic optimization results are used as the start point of the next steepest descent gradient optimization algorithm. Moreover, as the intensity of each light primary/LED is positive, positivity constraint was imposed on the optimizations. RMSE as shown in Eq. (9), was used as the fitness function of the optimization algorithms. In Eq. (9) n_w is the number of wavelength, $\mathbf{e}_i$ is the power of the desired illuminant in the i$^{\text{th}}$ wavelength and $\hat{\mathbf{e}}_i$ is the estimation of $\mathbf{e}_i$. The use of normalizing factor of $\frac{1}{n_w}$ in Eq. (9) is to make results independent of the number of the wavelengths.

$$\text{RMSE} = \sqrt{\frac{1}{n_w}\sum_{i=1}^{n_w}(\mathbf{e}_i - \hat{\mathbf{e}}_i)^2}. \tag{9}$$

Goodness of fit coefficient is another metric for the assessment of the reconstructions. This metric evaluates reconstructions as the cosine of the vector angle between the target and the reconstructed vector, as shown in Eq. (10). It is evident that a close reconstruction will give GFC of 1 while the worst GFC is 0.

$$\text{GFC} = \frac{\mathbf{e}^t.\hat{\mathbf{e}}}{||\mathbf{e}^t||.||\hat{\mathbf{e}}||}. \tag{10}$$

Although the spectral metrics of RMSE and GFC are the engine of the 3 proposed algorithms, for having a colorimetric view of the reconstructions, the two common colorimetric metrics of CRI [18] and CCT were also controlled for the spectral reconstructions. For the case of CCT, absolute difference of CCT of the reconstructed light with its companion target ($|\Delta\text{CCT}|$) was studied as a means to control the proximity of the correlated color temperatures as defined in

Optics EXPRESS

Eq. (11).

$$|\Delta CCT| = |CCT_{std} - CCT_{rec}|. \tag{11}$$

Where, CCT_{std} and CCT_{rec} are the correlated color temperature of the target standard illuminant and its reconstruction, respectively.

3.1. Implementation of the proposed algorithms using simulation with the imaginary light primaries

The aim of this section is to control the ability of the proposed algorithm for exploiting the potential of light emitting sources that are not available to the authors at the moment or might be developed in the future. To do so, 200 light primaries were generated using randomized weights of the function presented in Eq. (12).

$$y = \sum_{i=1}^{3} a_i.\exp\left(-\left(\frac{x - c_i}{b_i}\right)^2\right). \tag{12}$$

The form of Eq. (12) was selected so as to be able to simulate several single peak LEDs or multiple peaks OLEDs [7,9,13,19]. To control the diversity of the generated light primaries, the chromaticity diagram of the proposed light sources is presented in Fig. 3. As could be seen the generated light primaries are evenly distributed in the color space ranging from a white to the saturated ones.

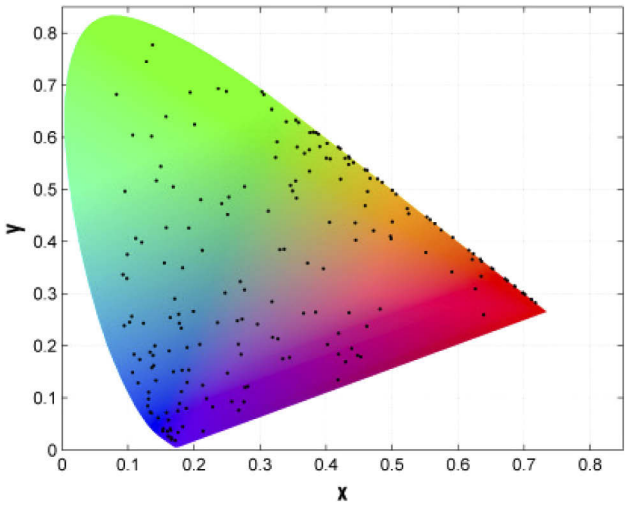

Fig. 3. Chromaticity diagram of the generated imaginary light primaries.

These light primaries were entered to the three proposed algorithms to select the best 15, 20, 25, 30 and 35 light primaries in order to control the performance of the 3 proposed selection algorithms.

3.2. Implementation of the proposed algorithms in simulation and practice using 40 real LEDs

40 LEDs were used in the current study as a set of available LEDs; 34 of them were from "Standard LEDs" category of Roithner Lasertechnik Gmbh with the specifications published in [20]. The six other were selected from available 5mm diameter LEDs at Tehran's electronics shops. The chromaticity and the SPD of the LEDs are shown in Fig. 4(a) and (b), respectively.

Optics EXPRESS

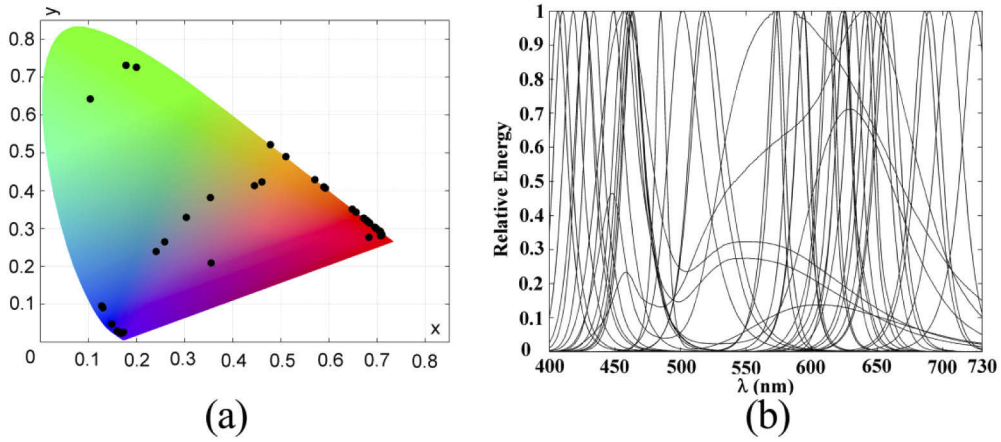

Fig. 4. Spectral power distribution of the available LEDs.

As the available 40 LEDs have emission peaks at about 400-730 nanometers, optimizations for matching of the target standard illuminants were performed assuming this wavelength range. This assumption will prevent wrong conclusions from the simulations, as the errors could grow beyond this wavelength range.

In order to omit goniometric dependencies of LEDs and to have complete mixed integrated light, an integrating sphere was made and used in the study. Moreover, for increasing the luminous power and symmetry as well as homogenous spreading of the light inside the sphere, two replicas of each aforementioned 40 LEDs, were mounted inside the sphere. In other words, 80 LEDs were mounted inside the sphere. The diameter of the integrating sphere was 35 cm and the inner walls were coated using the slurry of Barium Sulfate and an adhesive resin. LEDs were soldered on a 2 cm width ring-shaped PCB circuit and were connected to a board equipped with an ARM microcontroller using a 40 pin wire flat ribbon cable and then to a computer via a serial to USB convertor in order to be controlled via serial port in MATLAB. The microcontroller was programmed such that LEDs can be controlled using 8 bits data command. The pulse width modulation (PWM) technique was used for controlling intensity of the LEDs. In order to provide estimation of luminous intensity of the 40 LEDs in the integrating sphere, the maximum luminance values of LEDs are presented in Table 1.

3.2.1. Simulation using the 40 real LEDs

The spectral power distribution of the 40 LEDs were measured at their maximum power using Konica Minolta CS-2000 spectroradiometer from the viewing aperture of the integrating sphere. These SPDs were entered in to the three proposed algorithms to test them for the reconstruction of the studied standard illuminants.

3.2.2. 40 real LEDs in practice

In order to calibrate the LEDs, each pair of identical LEDs was lit up using different intensities (10, 30, 50, 70, 90, 110, 130, 150, 170, 190, 210, 230, 250 and 255) in an 8 bits system for the characterization of its optoelectronic behavior. Radiance of LEDs at each intensity was measured using Konica Minolta CS-2000 spectroradiometer from the viewing aperture of the integrating sphere.

Despite reports on the shifts in wavelength of maximum power at different levels of electrical current [9], almost zero shift (± 1 *nm*) was observed probably due to the extremely low power consumption of the studied LEDs. This indicates that the routine method of using power law

Optics EXPRESS

Table 1. Peak wavelengths and the maximum luminous intensity of the LEDs inside the integrating sphere.

LED no.	1	2	3	4	5	6	7	8	9	10
Peak wavelength	406	410	418	427	430	434	449	463	462	577
luminance (cd/m2)	0.22	0.13	0.18	0.59	1.5	1.26	2.25	4.87	6.05	0.1
LED no.	11	12	13	14	15	16	17	18	19	20
Peak wavelength	502	517	572	594	612	614	623	628	632	641
Luminance (cd/m2)	3.71	17.8	1.21	1.95	2.57	10.9	2.29	1.98	6.54	1.46
LED no.	21	22	23	24	25	26	27	28	29	30
Peak wavelength	644	655	651	658	687	690	705	725	519	596
luminance (cd/m2)	0.54	0.72	0.89	1.62	0.29	0.28	0.22	0.07	27.4	10.3
LED no.	31	32	33	34	35	36	37	38	39	40
Peak wavelength	625	588	464	white	white	white	white	white	white	pink
luminance (cd/m2)	10.8	3.33	9.02	2.48	6.24	27.1	20.1	14.2	2.45	1.27

between the output and the user control parameter for modeling the additive color devices can be implemented for the current problem [4,5,15]. The model is shown in Fig. 5(a) and Eq. (13). Taking logarithm function from both sides of the power law model, will result in linear model of LEDs relative optical emmitance as a function user controllable data (d_n) as is shown in Eq. (14).

$$\begin{aligned} &I_{\text{relative,nominal}} = \beta I^{\alpha}_{relative,real}, \\ &such\ that: I_{\text{relative,nominal}} = \frac{d_n}{255}. \\ &and \quad I_{relative,real} = \frac{I_{measured}}{I_{measured\ at\ d_n=255}}. \end{aligned} \tag{13}$$

$$\log(I_{\text{relative,nominal}}) = \alpha \log(I_{\text{relative},real}) + \log(\beta). \tag{14}$$

Where α and β are calculated via regression using an intensity ramp. $I_{\text{relative,nominal}}$ and $I_{relative,real}$ denote nominal relative intensity and the ground truth relative intensity of each LED, respectively. This model is named as Complete Logarithmic Regression (CLR) in this study.

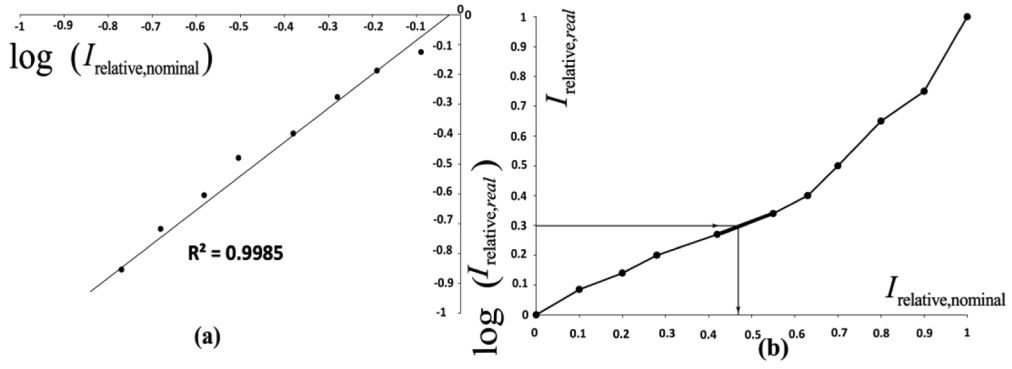

Fig. 5. Illustration of the two calibration methods.

The other method named Slice Linear Regression (SLR) was also applied. This method is based on drawing line between each successive point in the regression ramp. In this method user

Optics EXPRESS

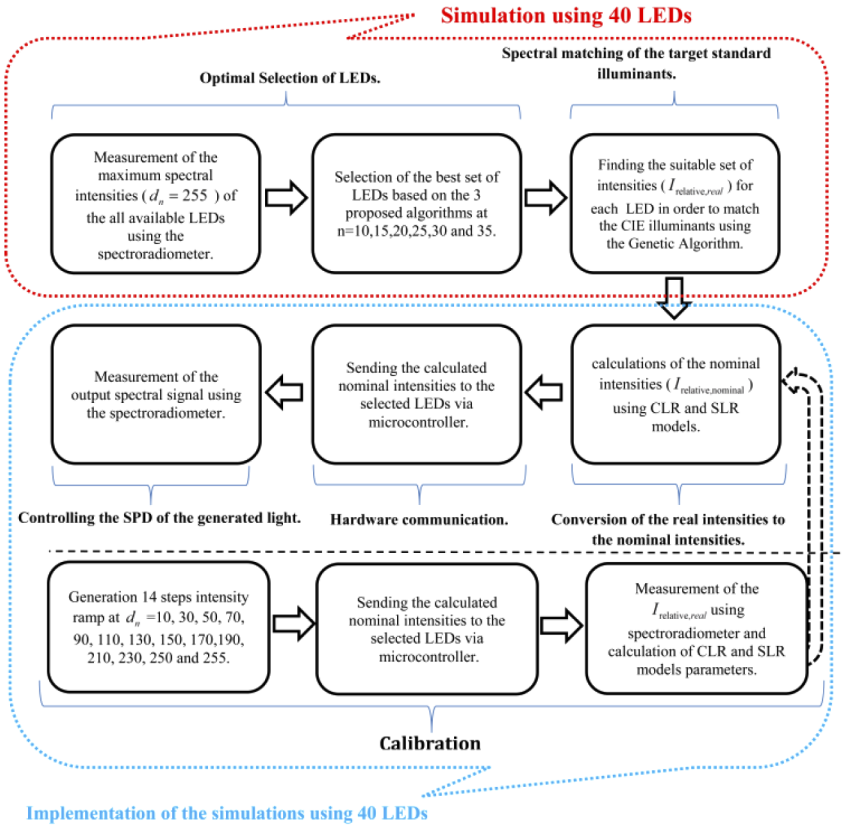

Fig. 6. Schematic illustration of the calibration, optimal selection, spectral matching and controlling the results using different numbers of LEDs.

controllable data for a desired relative intensity are estimated from the equation of corresponding piece of line connecting corresponding points (Fig. 5(b)).

Verification of the two calibration methods was done using comparison of theoretical matches of the light sources with their corresponding measurements in reality.

In order to make a clear view of the whole procedure, the flowchart of the steps is illustrated in Fig. 6. The upper rounded rectangular callout box in this figure shows section 3.2.1 in brief and the lower callout box is the illustration of section 3.2.2. It is evident that the details of the use of imaginary light primaries for selection and matching of the desired standard illuminants is much simpler than the use of real LEDs as linearization, calibration and controlling of the results stages does not exist. For the case of using imaginary light primaries the schematic diagram of the stages is shown in Fig. 7.

Optics EXPRESS

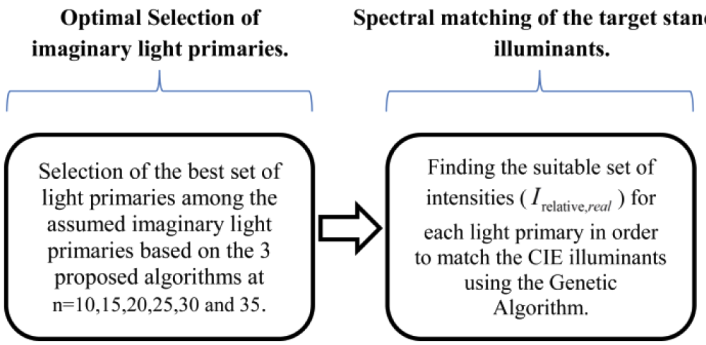

Fig. 7. Schematic illustration of using different numbers of imaginary light primaries for selection and matching the target standard illuminants.

4. Results and discussion

The three proposed LED selection methods were compared for the simulation of the 6 standard illuminants. For each method-illuminant combination, LED optimizations were done for 15, 20, 25, 30 and 35 optimally selected LEDs and the same was done for the light primaries. This was done to study the effect of the number of light primaries/LEDs on the quality of the optimizations. Processes were done using a laptop equipped with 2nd generation CPU of Intel core i5 2540M and 4 Gigabytes DDR3 RAM. The selections for each of the 15 (3*5) combinations of method-number of light primaries/LEDs took about 2-3 seconds. Optimizations for each of the 90 (3*6*5) method-standard illuminant-number of light primaries/LEDs combinations took about 4-8 seconds.

4.1. Simulation using imaginary light primaries

Results of the simulation of the six target standard illuminants using the three proposed methods exploiting different set of optimally selected light primaries in terms of RMSE, GFC, |ΔCCT| and CRI are presented in Fig. 8(a),(b),(c) and (d) respectively.

As could be seen from Fig. 8(a), RMSE of all the methods for every standard illuminants decreases as the number of primaries increases. However, the decease of the errors has leveled-off at 30 and 35 selected light primaries. For 15-20 selected primaries, the performance of the "Gram" and "Ortho" methods are almost the same but is better than that of the "Equal" method. For the 25-35 optimally selected light primaries, "Ortho" gives the best performance as compared to "Gram" and "Equal". The only exception in this trend is the illuminant "A" which is different in nature from the other 5 studied standard illuminants.

From the colorimetric metric point of view, in contrast to the spectral metrics, "Gram" shows better reconstructions than "Ortho" at 30 and 35 optimally selected primaries. This is the known paradox of losing spectral performance of the reflectance reconstructions at the expense of acquiring colorimetric metrics which has been solved using calorimetrically weighted least square techniques [21–23].

"Gram" method in theory, seeks the expansion in the spectral space. "Ortho" method, in contrast, searches for primaries which enable matching system to cover the standard illuminants. When the number of the primaries is low, as it is the case in the 15-20 selectable light primaries, expansion in the spectral space ("Gram") gives the same performance as maximizing the projection power of the target standard illuminants on to the light primaries ("Ortho"). By increasing the number of light primaries beyond 25, "Ortho" method performance exceeds that of the "Gram" method probably due to the higher capability of the "Ortho" in covering the spectral subspace spanned by the target standard illuminants. The trivial method of selection based on the

Optics EXPRESS

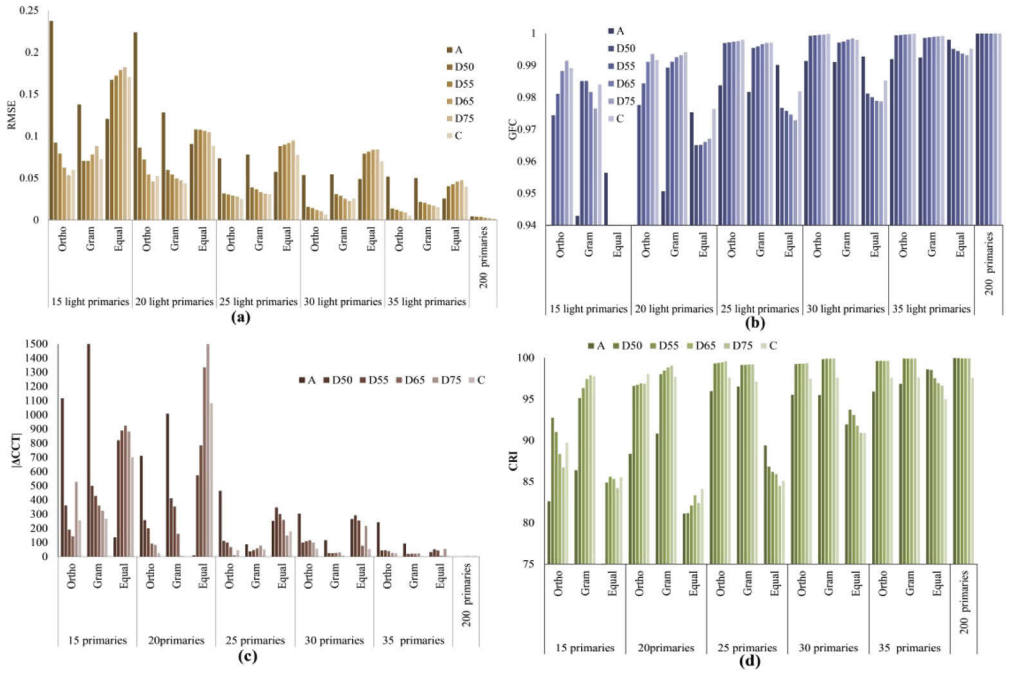

Fig. 8. Performance of the 3 proposed selection methods for 15, 20, 25, 30 and 35 selected light primaries. RMSE(a), GFC(b), |ΔCCT|(c) and CRI(d).

peak wavelength ("Equal") shows unsatisfactory performance except for the standard illuminant "A".

We believe that the unexpected answers of the standard illuminant "A" is due to the force of the Genetic algorithm optimization engine for lowering reconstruction error for all of the studied illuminants with the same weight. In other words, as the standard illuminants of the daylight series and "C" are somehow spectrally similar but completely different from the illuminant "A", optimizer's effort for lowering the error will ends in better performance for the daylight series but worse for the illuminant "A". For proving this claim, it can also be seen from Fig. 8(a) and (b) that the more close is the color temperature of the illuminants the more similar is the performance of the reconstructions. This implicitly confirms difference of the results for the standard illuminant "A".

4.2. Simulation using 40 real LEDs

Results obtained from the implementation of the 3 proposed algorithms on the 40 real LEDs are presented in Fig. 9. Similar to the imaginary primaries, for the selection of LEDs, the general trend in all the methods is the increase of spectral performance by increasing the number of LEDs. "All LEDs" in Fig. 9 indicates the highest performance that can be achieved in the optimizations with all available 40 LEDs. Surprisingly, from the spectral metric of RMSE point of view, the general trend in "Equal" method has been violated at 25 LEDs. "Equal" method has also lost some of its performance as the number of LEDs increases from 20 to 25 probably due to some double peak white LEDs existing in the available LED set. Meanwhile, the improvement of RMSE of the "Gram" method has stopped at 30 LEDs and shows approximately the same performance as "All LEDs".

Geometrically, "Gram" method looks for the maximum expansion in the spectral vector space via foundation of orthogonal bases. In the vector space generated by our 40 LEDs, each LED's

Optics EXPRESS

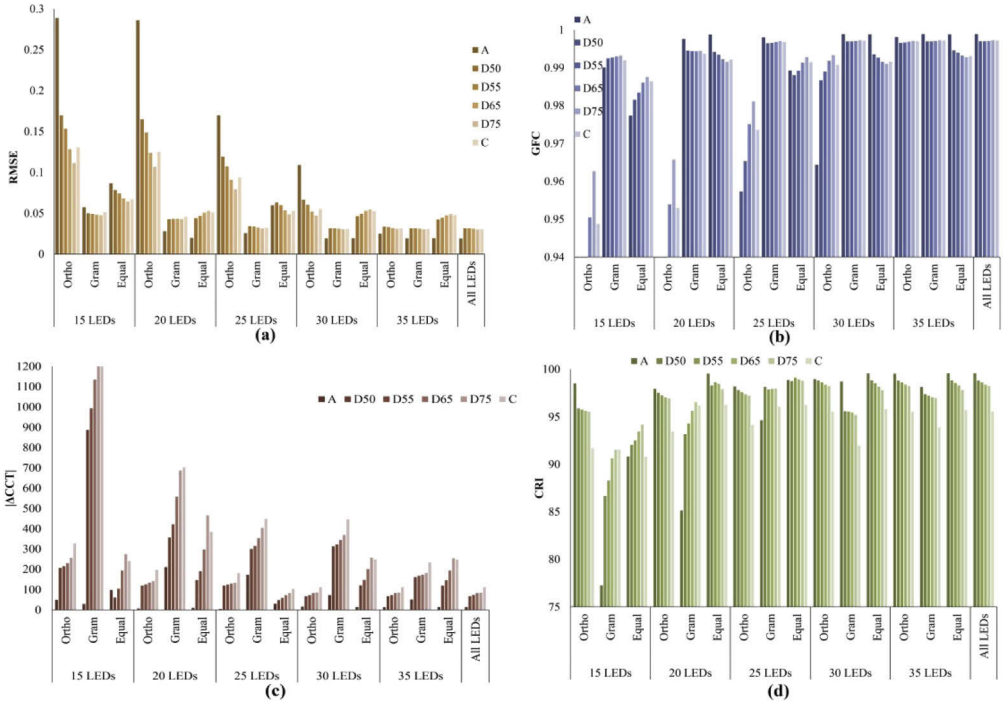

Fig. 9. Performance of the 3 proposed selection methods for 15, 20, 25, 30 and 35 selected LEDs. RMSE(a), GFC(b), |ΔCCT|(c) and CRI(d).

SPD is somehow mathematically orthogonal to the other SPDs as their dot product is close to zero as is quite the same for the LEDs selected based on "Equal" method. So this is quite understandable experiencing similar spectral performance behavior in "Gram" and "Equal" methods compared to "Ortho". Basically, "Ortho" looks for orthogonality of projection vectors of the standard illuminants on the selected LEDs vector space. In other words, it looks for vectors on which the illuminants subspace has the most different projections on them. Having different projections means fully spanning of the desired illuminants subspace and consequently lower simulation error. At 35 LEDs "Ortho" has reached its maximum power in covering the target standard illuminant via projections. This justification fits the simulations results in Fig. 9.

Similar to Fig. 8, the other interesting point in Fig. 9 is the similarity of the results for the illuminates with similar color temperature. This is due to the similarity of the targets in the spectral space.

The most noticeable difference between the results presented in Fig. 9 and Fig. 8 is the replacement of "Ortho" with "Gram" as the best method, from the spectral metrics point of view, especially at 25 and above primaries. While "Ortho" exhibited the best performance for imaginary light primaries in section 4.1, here "Gram" is the best for the real LEDs. We believe that this stems from the SPD of the set of available LEDs and the light primaries. The SPD of the LEDs are narrow and single peak while the SPD of imaginary light primaries are a mixture of single peak narrow band with single, double and triple peak narrow and wide band ones. Each pair of the selected LEDs among the available 40 LEDs in this study possesses acceptable degree of orthogonality. This is quite the opposite for the imaginary light primaries. It is evident that the criteria of steps of proposed progressive algorithms of "Gram" are fully satisfied for the narrowband LED case due to their mutual orthogonality.

Optics EXPRESS

4.3. Implementation of the simulations using 40 real LEDs

To examine the simulation results in reality and also obtain a tangible estimation of optimizations results, the results of the optimizations for the illuminants A and D50 were transformed into user controllable data using SLR and CLR methods. The generated SPDs were measured using the spectroradiometer. Results are shown in Table 2 and Fig. 10.

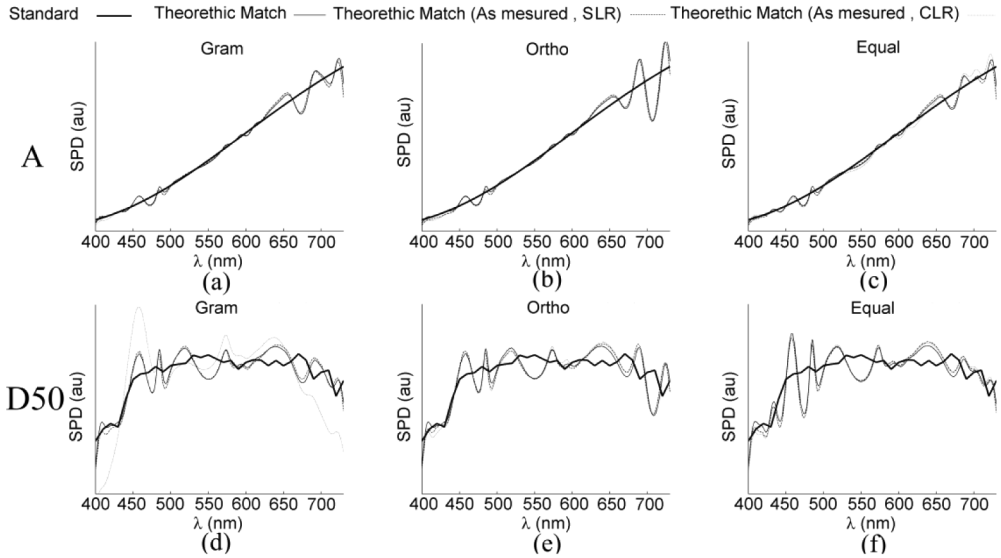

Fig. 10. Simulations (Theoretic Match) and true measurements (Theoretic Match-As measured) of the illuminants A (a, b and c) and D50 (d, e and f) using 35 optimally selected LEDs.

Table 2. luminous intensity (cd/m^2) of the reconstruction of standard illuminants A and D50 using 3 proposed algorithms with different calibration techniques.

	A		D50	
method	SLR	CLR	SLR	CLR
Gram	16.32	16.30	9.47	9.16
Ortho	16.20	16.04	9.40	9.42
Equal	16.38	16.31	26.16	26.16

In Fig. 10 results for the two illuminants of A and D50 (rows), along with the proposed selection algorithms (columns) are presented. The legend "Standard" refers to the standard illuminant, "Theoretic Match" is the simulation results of the optimization algorithm, while "Theoretic Match (as measured)"s show the implementation of the LEDs optimized weights in practice using CLR and SLR techniques.

Despite deviations from the "Standard"s, it is quite clear that the SLR method has been able to follow the "Theoretic Matche"s, while CLR method shows unwanted deviations from the "Theoretic Match"s. Considering the fact that CLR method minimizes the total residual errors, it is evident that, in some intensities, the prediction of the regression model have large difference from its training data which causes deviations in practice as can be seen in Fig. 10(d).

Moreover, it can be seen from Table 2 that the luminous intensities obtained using CLR and SLR calibration techniques are almost the same. This implies that the better performance of the SLR method is not due to the different error levels of error in locations of the calibration curves

Optics EXPRESS

of the LEDs, but it is due to its better predication power throughout all parts of the calibration curves.

5. Conclusion

Selection of LEDs for simulation of CIE standard illuminants are of great importance as they could generate more accurate simulations than their existing fluorescent simulators. However, selection of appropriate LEDs/light primaries would be tedious and cumbersome when plenty of them are available.

Using mathematical modeling of the problem three methods has been introduced for the selection. The methods "Equal" and "Gram", though different in mechanism, are the same in nature, specifically for the bell-shaped SPDs of the available LEDs in the market. The method "Ortho", as considers desired standard illuminants SPDs in the selection procedure, showed superior performance when larger numbers of light primaries are available.

According to the section 2, "Ortho" targets standard illuminants and tries to cover the standard illuminants subspace via most appropriate light primaries/LEDs. This is quite the opposite for "gram" and "Equal" methods. These two algorithms try to expand their spectral hyper volume in each selection steps, irrespective of the desired standard illuminants subspace. For the mutually spectral orthogonal light primaries/LEDs this expansion of spectral hyper volume is more successful than for the mutually spectral oblique light primaries/LEDs. The imaginary light primaries are a clear example of the latter light primaries/LEDs pairs while our real 40 LEDs epitomizes the former status.

It was shown as a rule of thumb that, the more selected LEDs the better performance of simulations. However, due to restrictions in number of light primary selections in the integrating spheres, and also the need for having blocks of simulating panels in the spectral light booths, up to 35 optimally selected LEDs/light primaries were investigated in this study. To summarize the findings the advantages and disadvantages of the proposed algorithms are listed in Table 3.

Table 3. Advantages and disadvantages of the three proposed algorithms.

	"Gram"	"Ortho"	"Equal"
Characteristics	Progressive expansion of the spectral subspace produced by the selected light primaries.	Progressive covering the desired standard illuminants subspace by the selected light primaries.	Selection of light primaries in different wavelength ranges.
Advantages	Good performance on imaginary light primaries.	Superior performance on imaginary LEDs.	Simplicity of the algorithms and implementation.
	Good performance on narrowband LEDs.	Good performance on narrowband LEDs.	
Disadvantages	Complexity of algorithm and implementation.	Complexity of algorithm implementation.	Not comparable performance on narrow band LEDs with "Gram" and "Ortho".
			Weak performance on imaginary light primaries.

Slice Linear Regression (SLR) showed promising performance for achieving the simulated light sources in reality. This might be due to the regression errors in some electrical current intensities that are neglected in the CLR calibration method.

It is worth noting that although luminous flux of the simulated lights are important; this problem can be easily solved in practice with replication of the light simulating blocks, providing each simulating block has a minimum needed flux. However, generalization of the proposed algorithms for simultaneously covering both metrics of luminous flux and RMSE is the aim of our future studies.

Optics EXPRESS

Disclosures

The authors declare no conflicts of interest.

References

1. I. Fryc, S. W. Brown, G. P. Eppeldauer, and Y. Ohno, "LED-based spectrally tunable source for radiometric, photometric, and colorimetric applications," Opt. Eng. **44**(11), 111309 (2005).
2. P. Bodrogi, T. Q. Khanh, and D. Polin, "Photopic Perceptual Aspects of LED Lighting," in *LED Lighting, Technlogy and Perception*, T. Q. Khanh, P. Bodrogi, Q. T. Vinh, and H. Winkler, eds. (Wiley-VCH Verlag GmbH & Co, 2015), p. 517.
3. "Light sources and illuminants" (Konica Minolta, 2019), retrieved 11th August, 2019, https://www5.konicaminolta.eu/en/measuring-instruments/learning-centre/light-measurement/light/light-sources-and-illuminants.html.
4. R. S. Berns, "A generic approach to color modeling," Color Res. Appl. **22**(5), 318–325 (1997).
5. R. Berns, Chap. "Optical Modeling of Colored Materials," in *Billmeyer and Saltzman's principles of color technology*, 3rd edition (Wiley, 2019), pp. 177–196.
6. E. Radkov, "White LEDs with tunable CRI," US Patent 7,768,189 B2 (Aug. 3, 2010 2010).
7. M. Mácha and S. Dušan, "Daylight Simulation based on real daylight LED module," in *21st International Conference LIGHT SVĚTLO*, (Brno, 2015), pp. 213–216.
8. B. Matusiak and T. Braczkowski, "Overcast sky simulator in the Daylight laboratory at NTNU, Trondheim," in *Visegrád*, (Hungary, 2014), pp. 1–7.
9. M. Mackiewicz, S. Crichton, S. Newsome, R. Gazerro, G. D. Finlayson, and A. Hurlbert, "Spectrally tunable LED illuminator for vision research," in *Conference on Colour in Graphics, Imaging, and Vision*, (Amsterdam, the Netherlands, 2012), pp. 372–377.
10. C.-C. Wu, N.-C. Hu, Y.-C. Fong, H.-C. Hsiao, and M. S.-L. Hsiao, "Optimal pruning for selecting LEDs to synthesize tunable illumination spectra," Light. Res. Technol. **44**(4), 484–497 (2012).
11. N.-C. Hu, C.-C. Wu, S.-F. Chen, and H.-C. Hsiao, "Implementing dynamic daylight spectra with light-emitting diodes," Appl. Opt. **47**(19), 3423–3432 (2008).
12. N.-C. Hu, Y.-C. Feng, C. Wu, and S. Hsiao, "Optimal radiant flux selection for multi-channel light-emitting diodes for spectrum-tunable lighting," Light. Res. Technol. **46**(4), 434–452 (2014).
13. J. Lei, G. Xin, and M. Liu, "Spectral assemblage using light emitting diodes to obtain specified lighting characteristics," Appl. Opt. **53**(35), 8151–8156 (2014).
14. A. Papoulis, "Moments and Conditional Statistics," in *Probability, Random Variables and Stochastic Processes*, S. W. Director, ed. (McGraw-Hill, 1991), p. 173.
15. J. Y. Hardeberg, "Acquisition and reproduction of colour images: colorimetric and multispectral approaches," (Ecole Nationale Supérieure des Télécommunications, Paris, France, 1999).
16. J. Y. Hardeberg, "Filter Selection for Multispectral Color Image Acquisition," J. Imaging Sci. Technol. **48**, 105–110 (2004).
17. J. E. Gentle, *Matrix Algebra, Theory, Computations, and Applications in Statistics*, Springer Texts in Statistics (Springer, 2007).
18. CIE, "Method of Measuring and Specifying Colour Rendering Properties of Light Sources," CIE 13.3 95 (Commission Internationale de L'éclairage, Vienna, 1995).
19. S. H. Han, Y. H. Park, and J. Y. Lee, "Design of High-Efficiency and Long-Lifetime White Organic Light-Emitting Diodes by Selective Management of Singlet and Triplet Excitons Using a Triplet Exciton Manager," Adv. Opt. Mater. **6**(24), 1800997 (2018).
20. R. L. Technik, "Diverse LEDs" (2020), retrieved 26th, July, 2020, http://www.roithner-laser.com/led_diverse.html.
21. B. Sluban, "Comparison of colorimetric and spectrophotometric algorithms for computer match prediction," Color Res. Appl. **18**(2), 74–79 (1993).
22. V. Babaei, S. H. Amirshahi, and F. Agahian, "Using weighted pseudo-inverse method for reconstruction of reflectance spectra and analyzing the dataset in terms of normality," Color Res. Appl. **36**(4), 295–305 (2011).
23. A. Mahmoudi Nahavandi, "Taking Full Advantage of RGB Sensor's Colorimetric Characteristics in Multi-Spectral Imaging," Prog. Color, Color. Coat. **13**(2), 121–130 (2020).